Jurnal Teknologi

ELECTROCHEMICAL PERFORMANCE OF ORDERED MESOPOROUS CARBON MODIFIED BY OXIDATIVE TREATMENT WITH AQUEOUS NITRIC ACID

Nur Izzatie Hannah Razman[a], Salasiah Endud[a*], Izan Izwan Misnon[b], Zainab Ramli[a]

*Corresponding author
salasiah@kimia.fs.utm.my

[a]Department of Chemistry, Faculty of Science, Universiti Teknologi Malaysia, 81310 UTM Johor Bahru, Johor, Malaysia
[b]Nanostructured Renewable Energy Materials Laboratory, Faculty of Industrial Sciences & Technology, Universiti Malaysia Pahang, 26300 Kuantan, Pahang, Malaysia

Graphical abstract
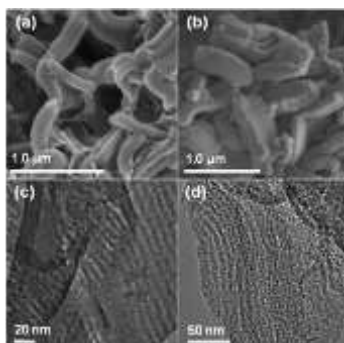
Abstract

In this study, ordered mesoporous carbon (OMC) was prepared via nano-casting method by using Santa Barbara Amorphous (SBA)-15 as a template and sucrose as a carbon precursor. The OMC was subsequently oxidized with aqueous nitric acid and referred as MOMC. The physicochemical properties of OMC and MOMC were determined using nitrogen adsorption–desorption analyser, field emission scanning electron microscopy (FESEM), transmission electron microscopy (TEM), and Fourier transform infrared spectroscopy (FT-IR). The results proved that the carbon replication process was successful. The electrochemical performance tests were carried out using cyclic voltammetry (CV) and galvanostatic charge–discharge (GCD) in 1 M KOH electrolyte for 1000 cycles. After oxidative treatment, the specific surface area and pore volume of OMC decreased but the specific capacitance of the electrode material has significantly increased from 117 F g^{-1} to 344 F g^{-1} at a scan rate of 10 mV s^{-1}.

Keywords: Ordered mesoporous carbon; SBA-15; template; oxidative treatment; electrochemical

Abstrak

Dalam kajian ini, karbon mesoliang bertertib (OMC) telah disediakan malalui kaedah penuangan-nano dengan menggunakan Santa Barbara Amorphous (SBA)-15 sebagai templat dan sukrosa sebagai pelopor karbon. OMC kemudiannya dioksida dengan asid nitrik akueus dan dirujuk sebagai MOMC. Ciri-ciri fizikokimia OMC dan MOMC ditentukan menggunakan penganalisis penjerapan–nyahjerapan nitrogen, mikroskop elektron pengimbas pancaran medan (FESEM), mikroskop pancaran elektron (TEM), dan spektroskopi inframerah transformasi Fourier (FT-IR). Keputusan kajian membuktikan bahawa proses replikasi karbon berjaya. Ujian prestasi elektrokimia telah dijalankan menggunakan voltammetri kitaran (CV) dan cas–nyahcas galvanostatik (GCD) di dalam elektrolit KOH 1 M untuk 1000 kitaran. Selepas rawatan oksidatif, luas permukaan spesifik dan isipadu liang OMC berkurang namun kapasitan spesifik bahan elektrod tersebut meningkat dengan ketara dari 117 F g^{-1} kepada 344 F g^{-1} pada kadar imbasan 10 mV s^{-1}.

Kata kunci: Karbon mesoliang bertertib; SBA-15; templat; rawatan oksidatif; elektrokimia

1.0 INTRODUCTION

There has been great interest in the development of ordered mesoporous carbon (OMC) material owing to its ordered pore structure, high specific surface area, large pore volume, chemical inertness, high mechanical stability and conductivity [1–2]. OMC can be prepared via nano-casting method which allows control of structure and morphology [3]. Generally, nano-casting method is a process in which a template with relevant nano-scale structure is impregnated with carbon precursor, and the initial template is subsequently removed [4]. The resulting carbon exhibits as mentioned criteria with variable three dimensional framework structures such as cubic and hexagonal, depending on the structure of the template. In other words, OMC prepared is usually a negative replicate of the used template. This method mainly used ordered mesoporous silica as template and sucrose or phenol resin as carbon precursor [5–6].

OMC material has been used in energy storage and electrochemistry applications due to its micropores which is essential for ions accumulation and well-aligned mesopores system (2–50 nm) which acts as highway for smooth electron and ions transportation [7]. However, the use of OMC materials as an electrode material for ideal electrochemical capacitor is mainly due to contribution of electrical double–layer capacitance, and the specific capacitance was less than 200 F g^{-1} [8].

Previous reports demonstrated that the application of this material is strongly influenced not only by its structural properties, but also by its surface functionalities. Oxygen surface functionalities (e.g., carboxylic acid, carbonyl, and hydroxyl) can be introduced by liquid phase oxidative treatment with nitric acid, hydrogen peroxide, or iron (III) nitrate. These oxygen surface functionalities are able to generate additional capacitance through faradaic reaction and recover the carbon surface hydrophilicity in aqueous electrolyte thus lead to improvement in electrochemical capacitive behaviour [9–10]. Therefore, it is of great interest to verify the influence of oxygen surface functionalities on the electrochemical performance of OMC materials.

In this study, OMC was prepared via nano-casting method by using SBA-15 as the template, followed by oxidative treatment with aqueous nitric acid. The as-synthesize OMC and oxidized OMC (MOMC) were characterized with respect to their morphological and structural properties and the electrochemical performance was investigated. The objectives of this study are to identify the differences observed in electrochemical behaviour of OMC and MOMC and clarify them in accordance to the role of oxygen surface functionalities.

2.0 EXPERIMENTAL

2.1 Materials

The Pluronic 123, tetraethyl orthosilicate (TEOS) and sucrose were purchased from Sigma–Aldrich, Germany. All other chemicals used for materials preparation and electrochemical testing were purchased from QReC™, Merck, Sigma–Aldrich and RCI Labscan Ltd., and used without further purification.

2.2 Synthesis of OMC and MOMC

SBA-15 template was prepared according to the procedure described by Zhao et al. [11]. Then, OMC was prepared via nano-casting method according to procedure described by Ryoo et al. [12]. The as-synthesize OMC was oxidized with 2 M HNO$_3$ aqueous solution at 80 °C for 2 h by reflux and the product obtained was referred as MOMC. For electrochemical performance testing, OMC and MOMC electrodes were prepared by mixing the samples (70 wt.%) with carbon (Super P, 15 wt.%) and PVDF binder (15 wt.%) by using NMP as a solvent. The mixture was stirred for 24 h and coated onto a pre-cleaned nickel foam substrate, heated at 60 °C for 24 h and finally pressed at 5 MPa.

2.3 Physicochemical Characterization of OMC and MOMC

The textural properties of OMC and MOMC such as specific surface area, pore volume, and pore size distribution were evaluated from nitrogen adsorption–desorption isotherms by using Micromeritics ASAP 2010 volumetric adsorption analyser. The specific surface area was determined from Brunauer–Emmet–Teller (BET) plot and pore size distribution was estimated by Barret–Joyner–Halenda (BJH) method from the desorption branch. TEM and FESEM images were obtained using JOEL microscopic instruments. The chemical species present after oxidative treatment was identified by Perkin-Elmer series 1600 FT-IR spectrometer.

2.4 Electrochemical Performance Tests

Cyclic voltammograms were obtained in the potential range of -1.0–0.0 V at various scan rates using three–electrode system using a potentiostat (Autolab PGSTAT 30, Eco Chemie B.V., The Netherlands). The gravimetric specific capacitance (C_S) of OMC and MOMC was calculated using the following equation:

$$C_S = \frac{1}{2mv\,(E_2 - E_1)} \int_{E_1}^{E_2} i(E)\,dE \qquad (1)$$

where m, v, E_2, E_1 and $i(E)$ are sample mass, potential scan rate, higher potential cutoff, lower potential cutoff, and current, respectively. Galvanostatic charge–discharge (GCD) was obtained by cycling the potential from -1.0 to 0.0 V with different current density. The specific capacitance (C_S) was also calculated from charge–discharge cycling using the equation:

$$C_S = \frac{it}{m\Delta V} \quad (2)$$

where i, t, m, and ΔV are constant discharge current, discharge time, sample mass, and open potential, respectively. All of the electrochemical measurements were performed using platinum as the counter electrode and Ag/AgCl as the reference electrode. Electrochemical performance of OMC and MOMC electrodes was compared in 1 M KOH electrolyte.

3.0 RESULTS AND DISCUSSION

3.1 Physicochemical Characterization of OMC and MOMC

The nitrogen adsorption–desorption isotherms of OMC and MOMC, as shown in Figure 1 (a) described typical type IV profile which is a characteristic of mesoporous materials [13]. This phenomenon is associated with capillary condensation in mesopores commenced at relative pressure $P/P_o > 0.42$. After oxidative treatment, BET isotherm studies showed decrease in specific surface area (S_{BET}) from 899.30 m^2 g^{-1} (OMC) to 551.10 m^2 g^{-1} (MOMC) and the pore volume decreased from 0.61 cm^3 g^{-1} (OMC) to 0.40 cm^3 g^{-1} (MOMC) for mesopores and decreased from 0.32 cm^3 g^{-1} to 0.21 cm^3 g^{-1} for micropores (seen in Table 1). The decrease in S_{BET} and pore volumes of MOMC may attributed to the introduction of oxygen surface functionalities over its pore wall and surface that caused pore disorientation or/and destruction on MOMC. Similar phenomenon has also reported by Cheah and co-workers on carbon coated monolith [14]. Besides, OMC shows H3 hysteresis loop, which does not exhibit any limiting adsorption at high P/P_o, representing aggregates of carbon particles with slit-shape pores [13]. After oxidative treatment, the MOMC shows similar loop shape but with narrower size.

Different structural parameters of OMC and MOMC were also observed from their pore size distributions calculated from BJH method, as presented in Figure 1 (b). The pore volume broad peaks centred at 4.10 nm and 4.45 nm for OMC and MOMC, respectively, suggests that the pore volumes are predominantly composed of mesopores and concentrated in a relatively wide size range. However, SBA-15 (data not shown) has larger pore size and better pore uniformity based on a much narrow and sharp capillary condensation step. This phenomenon occurred as OMC polymers undergo a substantial volume contraction and pore narrowing/broadening during

high temperature carbonization (800 °C) [15]. Nevertheless, the replication process of OMC from SBA-15 template was successful.
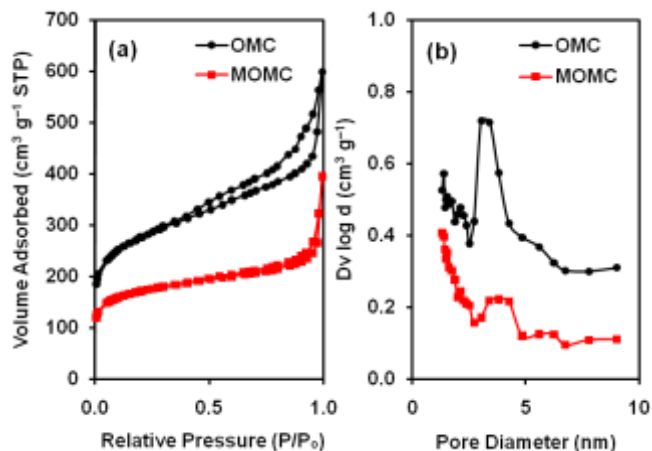

Figure 1 Nitrogen adsorption–desorption isotherms (a) and pore size distributions (b) of OMC and MOMC.

Table 1 Structural parameters of OMC and MOMC

Sample	^{a} S_{BET} (m^2 g^{-1})	^{b} V_{MESO} (cm^3 g^{-1})	^{c} V_{MICRO} (cm^3 g^{-1})	^{d} d_{BJH} (nm)
OMC	899.30	0.61	0.32	4.10
MOMC	551.10	0.40	0.21	4.45

^{a} Surface area determined from multi point BET analysis.
^{b} From the difference between the pore volume at $P/P_o = 0.97$ and V_{MICRO}.
^{c} From t plot (Harkins–Jura equation).
^{d} Calculated from desorption branch of the isotherm by BJH method.
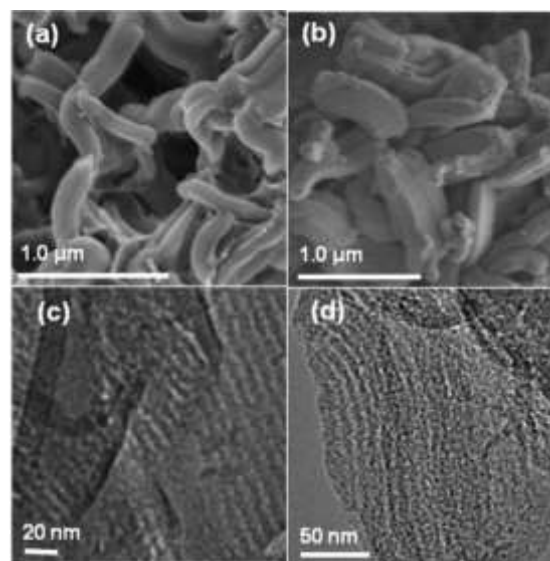

Figure 2 FESEM images of OMC (a) and MOMC (b); TEM images of OMC (c) and MOMC (d)

Figure 2 (a) and (b) are the FESEM images of OMC and MOMC. The images demonstrated short rod-like shape

particle morphology of OMC and MOMC with average length of 600–700 nm and 200–300 nm width. The obtained OMC had successfully retained the rod-like shape particle morphology of SBA-15 template, similar with previous study [6,16]. In addition Figure 2 (c) and (d), the TEM images of OMC and MOMC, respectively, exposed the presence of well-aligned mesopores channels with average width of less than 6 nm. From FESEM and TEM observation, we know that the ordered mesostructure structure of OMC was preserved after oxidative treatment and it is constant with nitrogen adsorption–desorption analysis data.
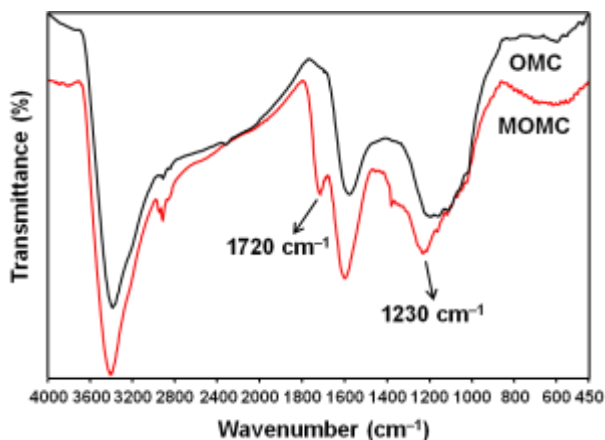

Figure 3 FT-IR spectra of OMC and MOMC

FT-IR spectra of OMC and MOMC are shown in Figure 3. Both samples exhibited two identical characteristic peaks at 3400 cm^{-1} and 1600 cm^{-1} corresponding to O–H group stretching and C=C stretching vibrations in graphene sheets, respectively. After oxidative treatment, two significant peaks appeared at 1720 cm^{-1} (C=O stretching vibration) and 1230 cm^{-1} (C–O vibration) indicated the existence of carboxyl groups. In addition, due to the usage of HNO_3, a weak absorption peak corresponding to NO_2 bending vibrations is observed around 1340 cm^{-1}. The –C=O and –C–O functional groups play an important role in enhancement of the carbon surface hydrophilicity as well as the electrochemical performance.

3.2 Electrochemical Studies

Figure 4 (a) and 4 (b) show CV profiles of OMC and MOMC electrodes at various scan rates (10, 25, 50, and 75 mV s^{-1}) in 1 M KOH electrolyte. The profiles comprise a series of approximately rectangular-like shape with a steep current change at the switching potential, which indicating electric double–layer capacitor behaviour. As the scan rates rises, both peak currents and peak–to–peak separation increased. The curves are able to preserve near rectangular shape as 75 mV s^{-1} is achieved, suggesting a highly reversible fast charging and discharging processes. After oxidative treatment, distortion of the CV curves becomes pronounce probably due to slow charging process induced by localization of electrons on the inhomogeneous MOMC

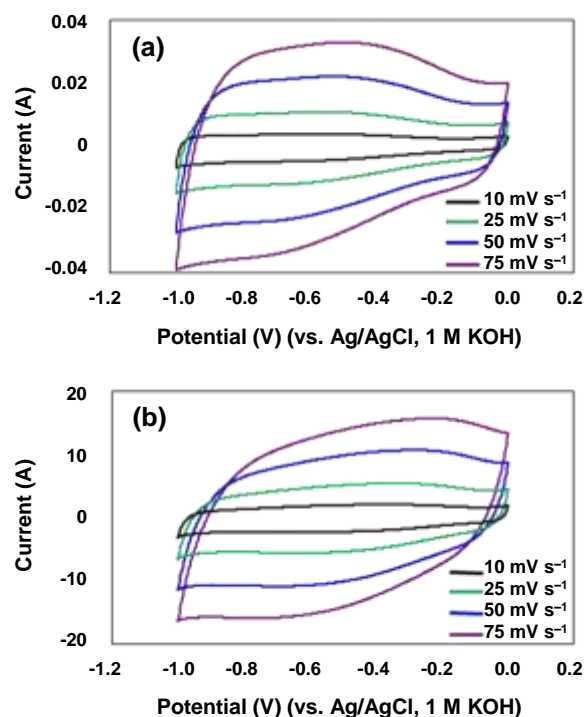surface [9]. The oxidative treatment also affects electronic resistance of the carbon materials [1,17].

Figure 4 Cyclic voltammograms of OMC (a) and MOMC (b) at 10, 25, 50, and 75 mV s^{-1} in 1 M KOH electrolyte

The specific capacitance (C_S) of OMC and MOMC was measured at various scan rates (10–150 mV s^{-1}) and the values are presented in Figure 5 (a). It can be clearly seen that the C_S of both electrode materials are strongly dependent on the scan rate. Specifically, the C_S decreases with increase in scan rate. The highest C_S was obtained at 10 mV s^{-1}. At all tested scan rate, MOMC exhibits higher C_S values compared to the OMC. The increment in C_S is an indicative of the pseudo-capacitance presence happened on the MOMC electrode interface, due to redox reactions of oxygen surface functionalities (–C=O and –C–O groups). However, when the scan rate increased from 10 mV s^{-1} to 150 mV s^{-1}, the C_S of OMC decreased 21% of its initial value. In contrast, the C_S of MOMC dropped by 35% from 344 F g^{-1} to 223 F g^{-1}. The drop percentage is higher than OMC probably contributed by distributed–capacitance effect and impaired conductivity after the oxidative treatment [9]. Improved hydrophilicity of the MOMC surface has also contributed to the capacitance improvement by favouring the electrolyte ions transportation to the micropores [7].

Charge–discharge analysis was conducted to determine C_S retention of OMCs electrodes in order for the electrodes to work steadily and safely. Figure 5 (b) shows the charge–discharge curves of OMC and MOMC at 0.5 A g^{-1}. The shape of the curves are not exactly linear, but show a typical triangle shape distribution which means that the materials have good double–layer electrochemical capability. MOMC experienced longer discharge time compared to OMC,

indicating a high charge–discharge propagation, low resistivity, and good reversible process [18]. The C_S of OMC and MOMC electrodes were summarized in Table 2. Worth to mention that the C_S of MOMC decreased to 146 F g^{-1} as the current density increased to 15 A g^{-1}, which proves its mass transportation efficiency and good charge–discharge rate [7].
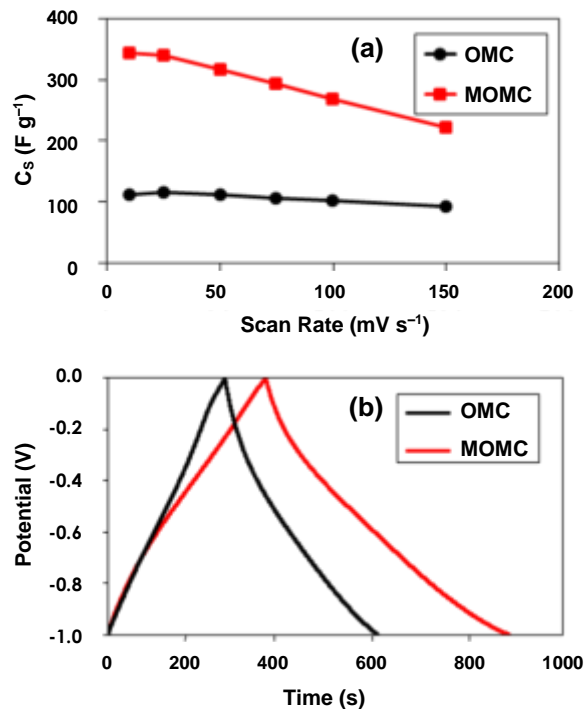

Figure 5 The specific capacitance (C_S) as a function of scan rate (a) and charge–discharge curves at 0.5 A g^{-1} (b) in 1 M KOH electrolyte

Table 2 Specific capacitance (C_S) for OMC and MOMC electrodes at various current densities (0.5–15 A g^{-1})

Samples	Specific Capacitance, C_S (F g^{-1})						
	0.5	1	3	5	7	10	15
OMC	153	142	128	122	117	111	101
MOMC	271	225	190	179	171	162	146

4.0 CONCLUSION

The electrochemical performance of OMC modified by oxidative treatment with aqueous nitric acid showed a significant improvement in specific capacitance (C_S) from 117 F g^{-1} (OMC) to 344 F g^{-1} (MOMC) due to contribution of pseudo-capacitance induced by faradaic reaction of oxygen surface functionalities (–C=O and –C–O groups). The C_S achieved a maximum value of 344 F g^{-1} at 10 mV s^{-1} and still remained a value of 222 F g^{-1} as the scan rate approaches 150 mV s^{-1}. The results proved that the oxidative treatment is suitable for OMC-based materials thus favouring its application as an electrode material for supercapacitor.

References

[1] Wu, X., Hong, X., Nan, J., Luo, Z., Zhang, Q., Li, L., Chen, H. and Hui, K. S. 2012. Electrochemical Double-Layer Capacitor Performance of Novel Carbons Derived from SAPO Zeolite Templates. *Microporous and Mesoporous Materials*. 160: 25–31.
[2] Matsui, T., Tanaka, S. and Miyake, Y. 2013. Correlation between the Capacitor Performance and Pore Structure of Ordered Mesoporous Carbons. *Advanced Powder Technology*. 24: 737–742.
[3] Saini, V. K., Andrade, M., Pinto, M. L., Carvalho, A. P. and Pires, J. 2010. How the Adsorption Properties Get Changed When Going from SBA-15 to Its CMK-3 Carbon Replica. *Separation and Purification Technology*. 75: 366–376.
[4] Gierszal, K. P., Jaroniec, M., Kim, T. -W., Kim, J. and Ryoo, R. 2008. High Temperature Treatment of Ordered Mesoporous Carbons Prepared by Using Various Carbon Precursors and Ordered Mesoporous Silica Templates. *New J. Chem.* 32: 981–993.
[5] Kruk, M., Jaroniec, M., Ryoo, R. and Joo, S. H. 2000. Characterization of Ordered Mesoporous Carbons Synthesized Using MCM-48 Silicas as Templates. *J. Phys. Chem. B.* 104: 7960–7968.
[6] Vinu, A., Srinivasu, P., Takahashi, M., Mori, T., Balasubramanian, V. V. and Ariga, K. 2007. Controlling the Textural Parameters of Mesoporous Carbon Materials. *Microporous and Mesoporous Materials*. 100: 20–26.
[7] Wu, X., Hong, X., Luo, Z., Hui, K. S., Chen, H., Wu, J., Hui, K. N., Li, L., Nan, J. and Zhang, Q. 2013. The Effects of Surface Modification on the Supercapacitive Behaviors of Novel Mesoporous Carbon Derived from Rod-Like Hydroxyapatite Template. *Electrochimica Acta*. 89: 400–406.
[8] Vix-Guterl, C., Frackowiak, E., Jurewicz, K., Friebe, M., Parmentier, J. and Béguin, F. 2005. Electrochemical Energy Storage in Ordered Porous Carbon Materials. *Carbon*. 43: 1293–1302.
[9] Li, H., Xi, H., Zhu, S., Wen, Z. and Wang, R. 2006. Preparation, Structural Characterization, and Electrochemical Properties of Chemically Modified Mesoporous Carbon. *Microporous and Mesoporous Materials*. 96: 357–362.
[10] Lufrano, F. and Staiti, P. 2010. Influence of the Surface–Chemistry of Modified Mesoporous Carbon on the Electrochemical Behavior of Solid-State Supercapacitors. *Energy Fuels*. 24: 3313–3320.
[11] Zhao, D., Huo, Q., Feng, J., Chmelka, B. F. and Stucky, G. D. 1998. Nonionic Triblock and Star Diblock Copolymer and Oligomeric Surfactant Syntheses of Highly Ordered, Hydrothermally Stable, Mesoporous Silica Structures. *J. Am. Chem. Soc.* 120: 6024–6036.
[12] Ryoo, R., Joo, S. H. and Jun, S. 1999. Synthesis of Highly Ordered Carbon Molecular Sieves via Template-Mediated Structural Transformation. *J. Phys. Chem. B.* 103(37): 7743–7746.
[13] Sing, K. S. W., Everett, D. H., Haul, R. A. W., Moscou, L., Pierotti, R. A., Rouquerol, J. and Siemieniewska, T. 1985. Reporting

Physisorption Data for Gas/Solid Systems with Special Reference to the Determination of Surface Area and Porosity. *Pure & Appl. Chem*. 57: 603–619.

[14] Cheah, W., Hosseini, S., Khan, M. A., Chuah, T. G. and Choong, T. S. Y. 2013. Acid Modified Carbon Coated Monolith for Methyl Orange Adsorption. *Chemical Engineering Journal*. 215–216: 747–754.

[15] Ignat, M. and Popovici, E. 2011. Synthesis of Mesoporous Carbon Materials *via* Nanocasting Route–Comparative Study of Glycerol and Sucrose as Carbon Sources. *Rev. Roum. Chim*. 56(10–11): 947–952.

[16] Fallah, A., Kordestani, D., Alizadeh, A. and Endud, S. 2013. Supported Palladium Catalysis Using a Biguanide N-Donor Motif on Mesoporous Silica for Suzuki–Miyaura Coupling Reaction. *Advanced Materials Research*. 622–623: 757–761.

[17] Fuertes, A. B., Pico, F. and Rojo, J. M. 2004. Influence of Pore Structure on Electric Double-Layer Capacitance of Template Mesoporous Carbons. *Journal of Power Sources*. 133: 329–336.

[18] Liu, X., Wang, Y., Zhan, L., Qiao, W., Liang, X. and Ling, L. 2011. Effect of Oxygen-Containing Functional Groups on the Impedance Behavior of Activated Carbon-Based Electric Double-Layer Capacitors. *J Solid State Electrochem*. 15: 413–419.